OncoImmunology

ISSN: (Print) (Online) Journal homepage: https://www.tandfonline.com/loi/koni20

# Oral administration of *Bifidobacterium breve* promotes antitumor efficacy via dendritic cells-derived interleukin 12

Qingxiang Li , Yuke Li , Yifei Wang , Le Xu , Yuxing Guo , Yixiang Wang , Lin Wang & Chuanbin Guo

**To cite this article:** Qingxiang Li , Yuke Li , Yifei Wang , Le Xu , Yuxing Guo , Yixiang Wang , Lin Wang & Chuanbin Guo (2021) Oral administration of *Bifidobacterium breve* promotes antitumor efficacy via dendritic cells-derived interleukin 12, OncoImmunology, 10:1, 1868122, DOI: 10.1080/2162402X.2020.1868122

**To link to this article:** https://doi.org/10.1080/2162402X.2020.1868122

ONCOIMMUNOLOGY
2021, VOL. 10, NO. 1, e1868122 (15 pages)
https://doi.org/10.1080/2162402X.2020.1868122

Taylor & Francis
Taylor & Francis Group

ORIGINAL RESEARCH

OPEN ACCESS Check for updates

# Oral administration of *Bifidobacterium breve* promotes antitumor efficacy via dendritic cells-derived interleukin 12

Qingxiang Li[a], Yuke Li[a], Yifei Wang[a], Le Xu[a], Yuxing Guo[a], Yixiang Wang[b], Lin Wang[a], and Chuanbin Guo[a]

[a]Department of Oral and Maxillofacial Surgery, Peking University School and Hospital of Stomatology, Beijing, China; [b]Department of Central Laboratory, Peking University School and Hospital of Stomatology, Beijing, China

**ABSTRACT**

Recent advances in immunotherapy, as a part of the multidisciplinary therapy, has gradually gained more attention. However, only a small proportion of patients who sensitive to the therapy could gain benefits. An increasing number of studies indicate that intestinal microbiota could enhance the efficiency of cancer immunotherapy. As one of the main probiotics, *Bifidobacterium* plays an important role in immune regulation, which has been proved by animal research and human clinical study. But the detailed mechanism was not clearly elucidated. Here we found oral administration of *Bifidobacterium breve* (*B. breve*) lw01 could significantly inhibit tumor growth and up-regulate tumor cell apoptosis, which relied on the recruitment of tumor-infiltrating lymphocytes and dendritic cells (DCs) in tumor microenvironment, but not *Lactobacillus rhamnosus* (*L. rhamnosus*) CGMCC 1.3724 or *Escherichia coli* (*E. coli*) MG1655. In the *in situ* ligated intestine loop model, *B. breve*'s stimulation triggered the upregulated expression of DC-related chemokine CCL20 and recruited more DCs in the intestinal villi. Further study revealed the enhancement of interleukin 12 (IL-12) secretion derived from DCs is essential to *B. breve*'s antitumor effect, which was counteracted by the treatment of neutralizing antibody for IL-12. Meanwhile, the modulation of intestinal microbiota caused by exogenous *B. breve* might enhance its antitumor effect. This study provides a simple and easy way to promote antitumor immunity via *B. breve*.

**ARTICLE HISTORY**
Received 31 August 2020
Revised 15 December 2020
Accepted 19 December 2020

**KEYWORDS**
*Bifidobacterium breve*; interleukin 12; dendritic cells; solid tumor; intestinal microbiota

## Introduction

Squamous cell carcinoma (SCC) is the most common malignancy of head and neck region.[1] Currently, multiple disciplinary team diagnosis and treatment model plays an important role in improving the survival and prognosis of head and neck squamous cell carcinoma (HNSCC) patients, which includes surgical excision and a combination of chemotherapy and/or radiotherapy.[2] Nevertheless, the 5-year survival rate for patients with HNSCC hasn't shown an obvious increase, which remains at 50% for several decades.[3] Therefore, major effects are being made to seek new therapies for gaining better clinical efficacy.

Growing evidence indicates that immunotherapy could enhance the host's immune surveillance to recognize tumor cells and halting or shrinking tumors via several approaches, including immune checkpoint blockade,[4–6] adoptive cell therapy,[7] and vaccines.[8] Tumor-infiltrating lymphocytes (TILs),[9] tumor neoantigens,[10] and patient microbiota[11,12] are reported to be the main factors influencing sustained tumor control derived from immunotherapy. However, most common cancer does not show abundant TILs, which consequently resulting in poor therapy efficiency. Intestinal microbiota, playing an important role in shaping immune system and mediating antitumor immune responses, are reported to be an alternative way to overcome these disadvantages.[12–15]

Since the association between gut microbiota and cancer immunotherapy gradually uncovered, some important cytokines and immune cells have been noticed. Interleukin 12 (IL-12), produced by inflammatory myeloid cells, is a kind of heterodimeric cytokines with proinflammatory properties.[16] IL-12 polarizes naive helper T cells (Th) to Th1 type and stimulates $CD8^+$ T cells and NKT cells.[17] Clinical studies based on IL-12 achieved well response, which mainly focused on local gene therapy.[18] Current studies indicated that IL-12 promoted the curative effect of CTLA-4 or PD-1 blockade[17,19,20] and adoptive cell therapy.[21] Dendritic cells (DCs) are important source of endogenous IL-12. It was reported that effective anti-PD-1 immunotherapy requires intratumoral DCs-derived IL-12.[19] And conventional type 1 DCs-derived IL-12 was necessary to the priming of follicular helper T cells, which was vitally important for the efficacy of chemotherapy for proximal colon cancer.[22] All these evidence suggest the crucial role of IL-12 in immunotherapy against solid tumor.

Although some specific bacteria, including *Akkermansia muciniphila*,[23] *Prevotella, Oscillibacter*,[24] and *Bifidobacterium*,[25] have been thought to play important roles in modulating cancer immunotherapy, the detailed mechanism was still far from elucidated, especially in extraintestinal tumors. *Bifidobacteria* are one of the pioneering colonizers of the early gut microbiota, and

**CONTACT** Lin Wang linwang911@126.com Department of Oral and Maxillofacial Surgery, Peking University School and Hospital of Stomatology, , Beijing 100081, P.R.China; Chuanbin Guo guodazuo@sina.com.

Supplemental data for this article can be accessed on the publisher's website.

they are known to play crucial role in the maturation of host's immune system.[26,27] It was proved that *Bifidobacteria* could regulate host immunity,[28] modulate immune responses,[29] relieve allergy symptoms,[30] treat inflammatory diseases,[31] and even possess synergistic action for tumor immunotherapy.[25] In the previous study from our group, *B. breve* held partial antitumor effect compared with the genetically-modified strain by tail vain injection.[32]

In this study, we chose HNSCC, the most common solid tumor in head and neck region as disease model. We evaluated the efficacy and explored detailed mechanisms of *B. breve* on HNSCC in mice by oral administration. *Lactobacillus rhamnosus* (*L. rhamnosus*) and *Escherichia coli* (*E. coli*) were chose as control bacteria. We put more efforts on the mechanism investigation including intestinal DCs modulation, IL-12 secretion and TILs alteration. Moreover, we also investigated the modulation of gut microbiota caused by exogenous *B. breve*.

## Methods

### Cell lines and culture condition

SCC VII murine cell line was obtained from Central Laboratory of Peking University School and Hospital of Stomatology. CT26.WT murine cell line was purchased from National Infrastructure of Cell Line Resource, China (Beijing). Both of them were cultured in Dulbecco's Modified Eagle Medium (DMEM) supplemented with 10% fetal bovine serum (Sigma-Aldrich), 100 IU/mL Penicillin and 100 μg/mL Streptomycin (Gibco) in a humidified atmosphere containing 5% $CO_2$/95% air at 37°C.

### Bacteria and culture condition

*Bifidobacterium breve* lw01 was isolated by our group previously,[33] and was routinely cultured in MRS Broth (BD) plus Raffinose (Amresco) supplement and 0.5% L-cysteine·HCl (Sigma-Aldrich), under anaerobic environment at 37°C. *Lactobacillus rhamnosus* CGMCC 1.3724 was purchased from the China General Microbiological Culture Collection Center (CGMCC), and was routinely cultured in MRS Broth (BD) plus Raffinose (Amresco) supplement under anaerobic environment at 37°C. *Escherichia coli* MG1655 strain, purchased from Wuhan Miaoling Bioscience & Technology Co. Ltd, was routinely cultured in Luria-Bertan Broth at 37 °C with vigorous shaking.

### Animals and tumor models

C3H/HeN mice and BALB/c mice, 6 weeks old, were purchased from Beijing Vital River Laboratory Animal Technology Co., Ltd. All mice were maintained under specific pathogen-free conditions. C3H/HeN mice were injected subcutaneously with $3 \times 10^6$ SCC VII cells, and BALB/c mice were injected subcutaneously with $5 \times 10^5$ CT26.WT cells. Tumor size was measured and determined as (length × width$^2$)/2. *B. breve, L. rhamnosus, E. coli* ($1 \times 10^9$ in 100 μL PBS) or PBS were given to mice in experimental or control group. All animal studies (including the mice euthanasia procedure) were done in compliance with the regulations and guidelines of Peking University Institutional Animal Care and Use Committee (LA2016276). Formula of tumor suppression rate was (A-B)/A*100%, where A and B were mean of tumor volume or weight from control and experimental group.

### In vivo IL-12 blocking treatment

Mice received 3 doses (once a week) of 1 mg of neutralizing antibody for IL-12 (R2-9A5, BE0233, BioXcell) or isotype control IgG2b (LTF-2, BE0090, BioXcell) via intraperitoneal injection.

### T cell depletion

For depletion of $CD4^+$ and $CD8^+$ T cells, mice were injected intraperitoneally weekly with rat *InVivo*MAb anti-mouse CD4 (GK1.5, BE0003-1, BioXcell) and rat *InVivo*MAb anti-mouse CD8α (53–6.7, BE0004-1, BioXcell), or isotype control IgG2b (LTF-2, BE0090, BioXcell) and IgG2a (2A3, BE0089, BioXcell) at a dose of 250 μg per mouse. These regimens resulted in > 99% depletion of $CD4^+$ and $CD8^+$ T cells from the peripheral blood, as evaluated by flow cytometry (supplementary figure S1a).

### Ligated loop experiments

Mice were anesthetized with pentobarbital sodium (80 mg/kg body weight, intraperitoneal). Terminal ileal ligated loop[34] was injected with *B. breve, L. rhamnosus, E. coli* ($1 \times 10^9$ in 100 μL PBS) or PBS. After 45 min, intestines were removed for qRT-PCR, ELISA, immunofluorescence, and immunohistochemistry staining.

### TUNEL assay

Tumor tissues were embedded in OCT (Tissue Tek). Cryosections at a thickness of 6 μm were cut by using a cryostat (Leica CM1900 UV) and were stained with *In Situ* Cell Death Detection kit (Roche) following the instruction. Visualization was performed using a fluorescence microscope (Olympus BX53). Five representative fields separated over the tumor tissue were randomly selected for statistical analysis.

### Western blot

Supernatant of tumor tissues was quantitated by BCA assay and 80 μg of protein was performed as reported before.[32] The following antibodies were used: anti-Bcl-2 (D17C4), anti-Bax (D3R2M), anti-Caspase-3 (8G10) from CST, and anti-β-actin (8H10D10) from Absin.

### Histology and immunohistochemistry

The isolated tumor tissues or small intestines were fixed, embedded, and sectioned at a thickness of 4 μm. Sections were deparaffinized, rehydrated, and then stained routinely with hematoxylin and eosin.

For immunohistochemistry, following antibodies were used: anti-IL-12A (ab203031), anti-IFN-γ (ab9657) from Abcam, anti-CD3ε (D4V8L), anti-CD4 (D7D2Z), anti-CD8α (D4W2Z) from CST. All the samples were detected by a microscope (Olympus BX53). Five representative fields separated over the tumor tissue were randomly selected for statistical analysis.

### Immunofluorescence and confocal microscopy

Cryosections of tumor tissues or small intestines were incubated with the primary antibodies and fluorescent secondary antibodies. The following antibodies were used: anti-CCL20 (ab9829) from Abcam, anti-CD11 c (D1V9Y) from CST, and goat anti-rabbit IgG H&L secondary antibodies from Zsbio. The cryosections were visualized by a fluorescence microscope (Olympus BX53). Five representative fields separated over the tumor tissue were randomly selected for statistical analysis.

### Flow cytometry

Single-cell suspension was prepared from the fresh tumor tissues by using mechanical trituration method and from the fresh ileal lamina propria by using enzyme digestion method. The following antibodies were used: FITC-CD4 (RM4-5), PE-CD3ε (145–2 C11), APC-CD8α (53–6.7), APC-CD45(30-F11), PE/Cy7-CD11c (N418), BV510-I-A/I-E (M5/114.15.2), BV421-CD103 (2E7), APC/Cy7-CD11b (M1/70), PE-IL-12p40 (C15.6) and respective isotype controls from BioLegend. Analysis was performed by using a flow cytometer (DxP Athena, Cytexbio).

### qRT-PCR

Total RNA was extracted from tissues or cells by TRIzol method. Quantification of mRNA expression was performed using FastStart Universal SYBR Green Master (ROX) reagent (Roche) on an ABI Step One Plus Real-Time PCR System. Sequences of the primers are shown in supplementary table 1.

### ELISA

Tissue supernatant of tumor or small intestine or culture supernatant of BMDCs was collected. IL-12 p70 level was determined by ELISA (BioLegend). The absorbance was measured using a microplate reader (Elx808; BioTek).

### BMDC generation and cell stimulation

Bone marrow (BM) cells were harvested from femurs and tibiae of C3H/HeN mice, and then cultured in RPMI-1640 medium (Gibco) containing 10% fetal bovine serum (Sigma-Aldrich), 100 IU/mL of Penicillin and 100 μg/mL of Streptomycin (Gibco), in the presence of 25 ng/mL rmGM-CSF and 12.5 ng/mL rmIL-4 (BioLegend) for 8 days at 37°C with 5% $CO_2$. BMDCs were then stimulated for 4, 8 or 24 hours without or with *B. breve, L. rhamnosus* or *E. coli* at a ratio of 1:100.

### B. breve quantitation of cecal contents

Cecal contents of mice were collected. DNA was extracted from each sample using TIANamp Stool DNA Kit (Tiangen). The V3-V4 region of the *B. breve* 16S ribosomal RNA gene was amplified by PCR using primers BreF 5′-CCGGATGCTCCATCACAC-3′ and BreR 5′-ACAAAGTGCCTTGCTCCCT-3′ with 50ng gDNA template.

### Bacterial identification in cecal contents

Cecal contents of mice were collected and frozen at −80°C. DNA extraction, Library construction and sequencing were conducted at Beijing Allwegene Technology Co., Ltd. (China). Operational Taxonomic Units were clustered using UPARSE (http://drive5.com/uparse/) and chimeric sequences were identified and removed using Usearch (version 7.0.1090). OTU profiling table and alpha diversity analyses were also achieved by python scripts of QIIME (version 1.9.1).

### Statistical analysis

The statistical analysis of tumor-growth curve in Figures 1(a), 6(a), S1b and S2a were performed by GraphPad Prism 7 with two-way ANOVA. The other statistical analysis in Figures 1–7 were performed with one-way ANOVA. The statistical analysis in Figure 8 is performed with two-tailed Student's *t* test. Values of $P < .05$ were considered to be statistically significant.

## Results

### B. breve exerted antitumor effect by oral administration

The antitumor effect was evaluated after *B. breve, L. rhamnosus* or *E. coli* administration orally by monitoring tumor volume and weight. Compared with control, *L. rhamnosus* or *E. coli* gavage group, *B. breve* gavage group showed significant tumor inhibition effect (Figure 1(a,b)). The tumor suppression rate calculated by volume or weight were 36.90% and 35.55%, respectively. TUNEL assay displayed more apoptotic cells (mean = 25.64 ± 8.649) in tumor tissues treated with *B. breve* compared to the other groups (mean = 8.012 ± 2.262, 12.04 ± 3.555 and 10.01 ± 2.163, Figure 1(c)). Consistent with this, the expression levels of pro-apoptotic protein cleaved caspase-3 and the ratio of Bax/Bcl-2 were increased only in *B. breve* gavage group (Figure 1(d)). These results suggested that oral administration of *B. breve* possess distinct antitumor effect compared with *L. rhamnosus* or *E. coli*.

### Orally taken B. breve influenced the pattern of tumor-infiltrating T lymphocytes

Compared with normal C3H/HeN mice, the antitumor effect vanished because of T cell depletion (supplementary figure S1). To confirm whether orally taken *B. breve* can trigger antitumor immunity via T cells, we analyzed the tumor-infiltrating lymphocytes (TILs) in tumor-bearing C3H/HeN mice model. As shown in Figure 2(a), there were significantly more $CD3^+$, $CD4^+$, and $CD8^+$ T cells (mean = 76.57 ± 15.63, 46.70 ± 14.13 and 49.57 ± 9.214) in the tumor tissues after

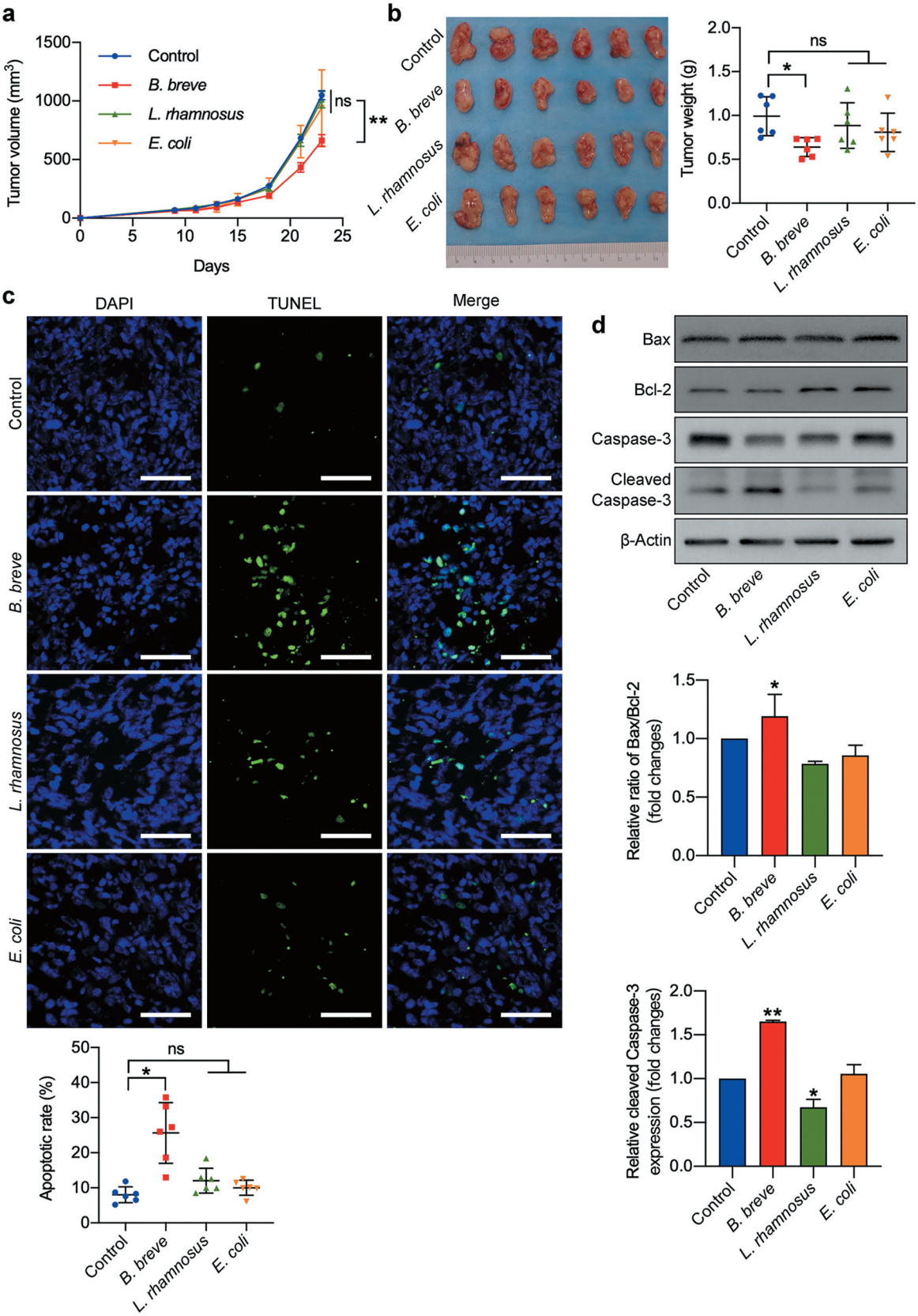


**Figure 1. Oral administration of *B. breve* induced tumor cell apoptosis and inhibited tumor growth**. C3H/HeN mice were subcutaneously injected with $3 \times 10^6$ of SCC VII cells. **a**. Tumor growth in C3H/HeN mice treated with PBS (control), orally taken *B. breve* ($1 \times 10^9$/mouse), *L. rhamnosus* ($1 \times 10^9$/mouse) or *E. coli* ($1 \times 10^9$/mouse) every other day from day 7. The data was presented as mean ± SEM. **b**. After administration for 2 weeks, the tumors were excised (left), and the tumor weight was shown in right. **c**. Apoptosis of tumor tissues from C3H/HeN mice was assayed with TUNEL staining and observed under fluorescence microscope (scale bar: 50 μm). The quantitative analysis of apoptotic tumor cells was performed by ImageJ software and presented in bar charts. **d**. The expression levels of Bax, Bcl-2, Caspase-3, and cleaved Caspase-3 in tumor tissues from C3H/HeN mice were checked by western blot assay. Densitometric analysis of protein expression was performed by ImageJ software and presented in bar charts (n = 2/group). Each dot represents one mouse in two to three independent experiments of six mice per group. Data in **b** and **c** presented as mean ± SD. Statistics were two-way ANOVA for tumor-growth curve (a) and one-way ANOVA to compare four independent groups (**b, d**; $^*P < .05$; $^{**}P < .01$; ns, not significant).

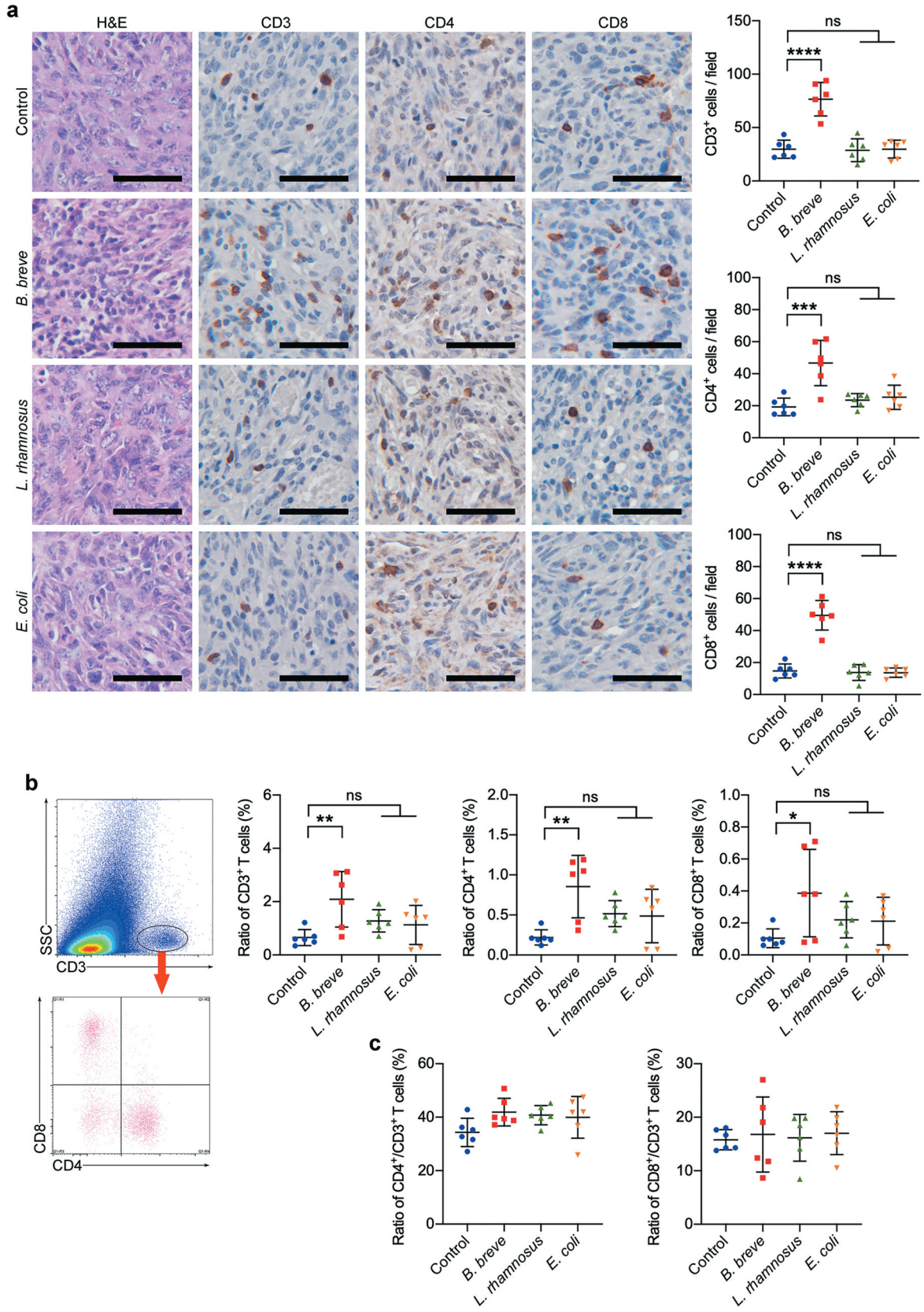


**Figure 2. Tumor suppression effect depended on antitumor immunity. a**. Representative H&E staining images of tumor tissues were shown in the left panel, and the expressions of CD3, CD4, and CD8 in tumor tissues were detected by immunohistochemical staining assay (left; scale bar: 50 μm). The quantitative analysis was performed by ImageJ software and the number of positive cells were presented in scatter plots (right). **b**. Representative plots showing gating strategy of $CD3^+$, $CD4^+$, and $CD8^+$ T cells within the tumor of C3H/HeN mice, as assessed by flow cytometry (left). The statistical analysis was shown in scatter plots (right). **c**. The ratio of tumor infiltrating $CD4^+/CD3^+$ T cells and $CD8^+/CD3^+$ T cells based on the data in **b**. Each dot represents one mouse in two to three independent experiments of six mice per group. All these data were analyzed with one-way ANOVA and presented as mean ± SD (*$P < .05$; **$P < .01$; ***$P < .001$; ****$P < .0001$; ns, not significant).

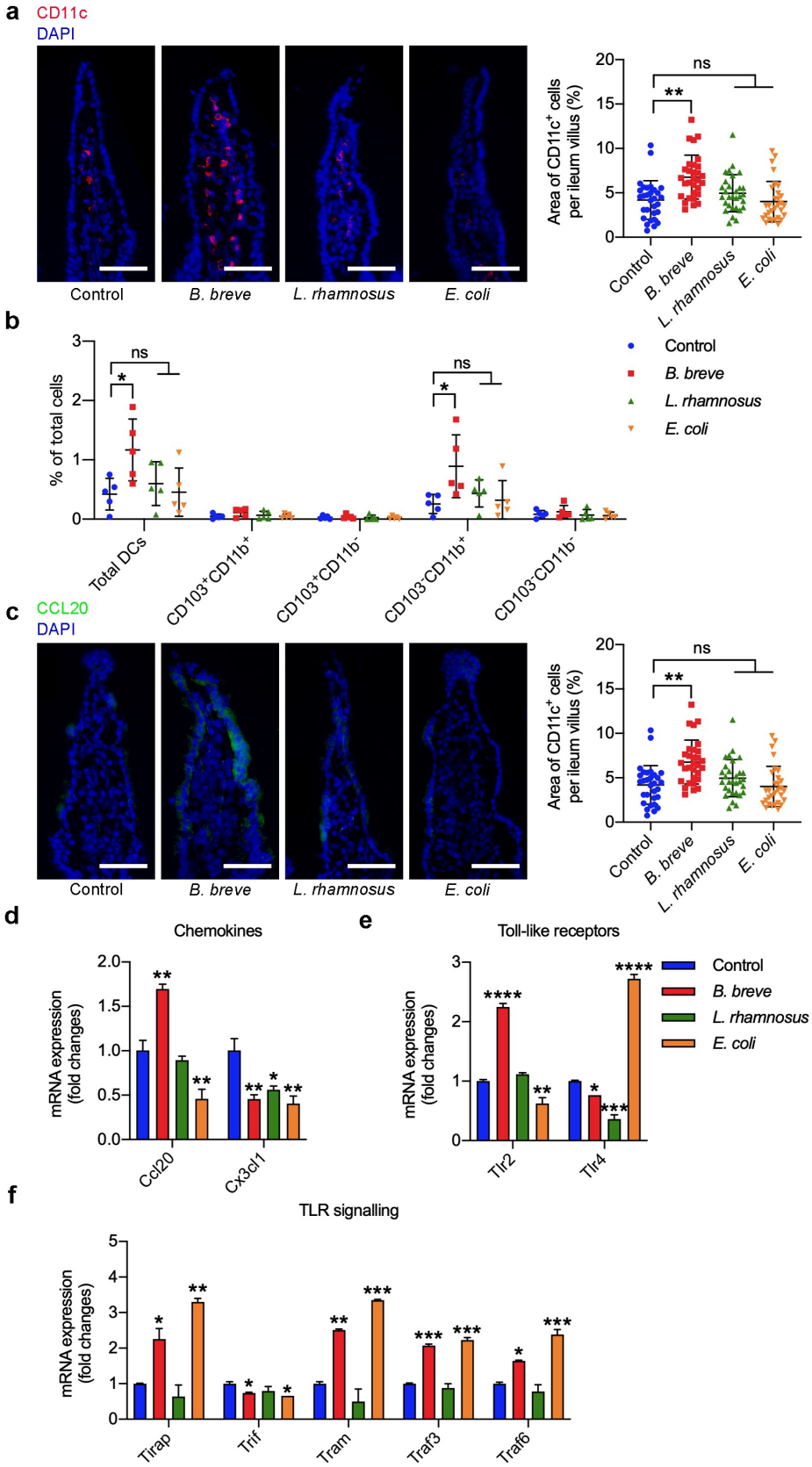


**Figure 3.** ***B. breve*** **primed intestinal DCs recruitment and maturation**. Ligated loops of C3H/HeN mice were injected with PBS, *B. breve, L. rhamnosus* or *E. coli* for 45 min. **a**. Cryosections of the terminal ileum were stained with CD11c (red) and DAPI (blue) and representative images were shown in (left). The quantitative analysis was performed by ImageJ software and the number of positive cells were presented in scatter plots (right). Each dot represents one ileum villus in two independent experiments of six mice per group. **b**. Flow cytometric analyses of total DCs ($CD11c^{+}MHC\text{-}II^{hi}$) and the subpopulations in ileal lamina propria from C3H/HeN mice. Each dot represents one mouse in two independent experiments of five mice per group. **c**. Cryosections were immunostained for CCL20 (green) and DAPI (blue). The quantitative analysis was performed by ImageJ software and the area of positive cells were presented in scatter plots (right). Each dot represents one ileum villus in two independent experiments of six mice per group. **d**. Relative mRNA expression level of the intestinal DCs-related chemokine CCL20 and CX3CL1 were evaluated by qRT-PCR. **e**. Relative mRNA expression level of the main intestinal epithelial Toll-like receptors was evaluated by qRT-PCR. **f**. Relative mRNA expression level of the key molecules in TLR signaling were evaluated by qRT-PCR. All these data were analyzed with one-way ANOVA and presented as mean ± SD (scale bar: 50 μm; *$P < .05$; **$P < .01$; ***$P < .001$; ****$P < .0001$; ns, not significant).

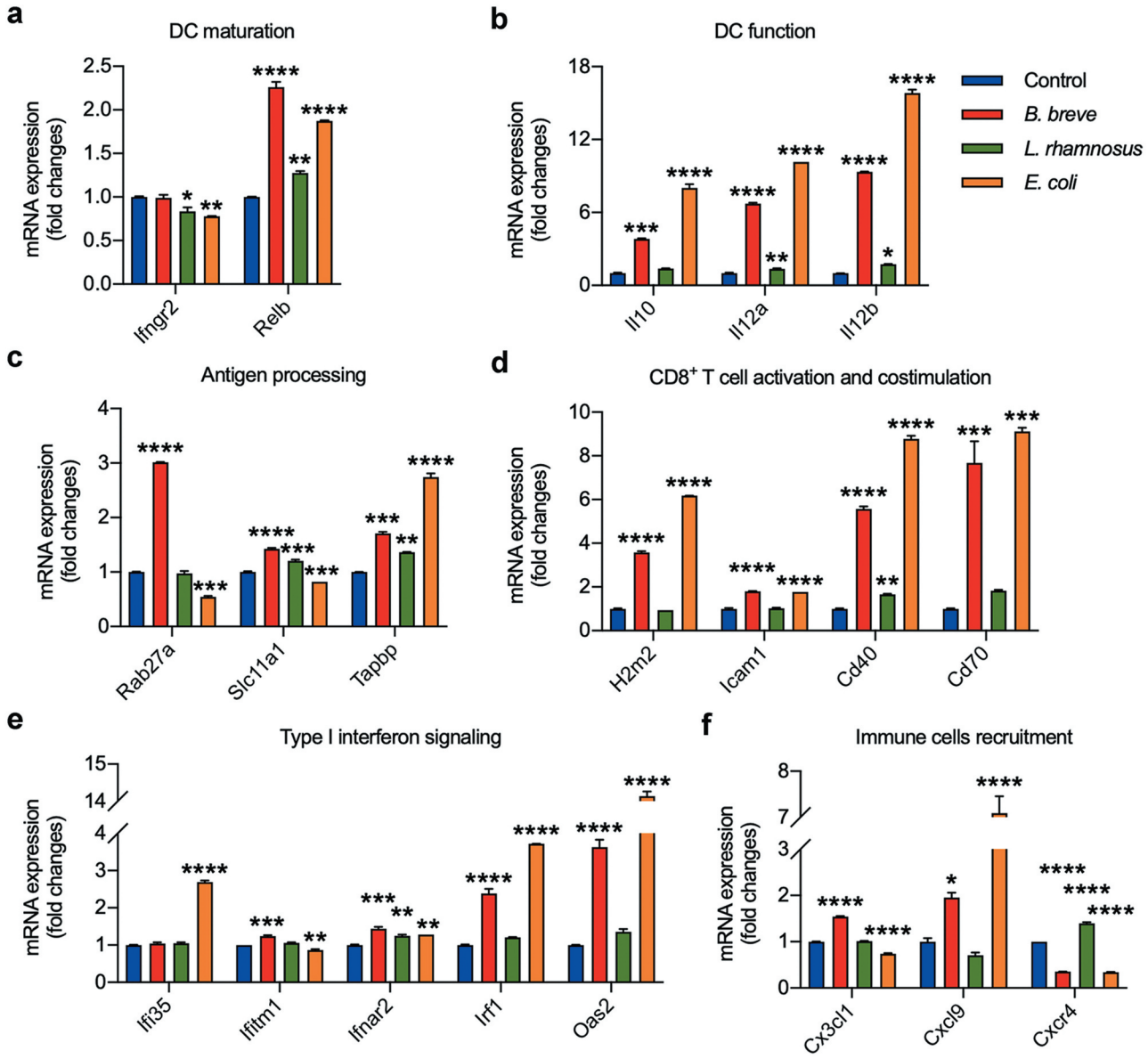


**Figure 4.** ***B. breve* enhanced BMDCs development and maturation in vitro**. BMDCs were stimulated for 4 hours with medium alone or with *B. breve, L. rhamnosus* or *E. coli* containing medium at a ratio of 1:100 BMDCs to bacterial cells. Relative mRNA expression level of key antitumor immunity genes in DCs were evaluated by qRT-PCR, which were crucial in DC maturation (a), DC function (b), antigen processing (c), $CD8^+$ T cell activation and costimulation (d), type I interferon signaling (e), and immune cell recruitment (f). All these data were analyzed with one-way ANOVA and presented as mean ± SD (*$P < .05$; **$P < .01$; ***$P < .001$; ****$P < .0001$).

*B. breve* administration than control group (mean = 29.83 ± 8.483, 19.27 ± 5.493 and 14.80 ± 4.365), *L. rhamnosus* group (mean = 28.77 ± 10.73, 23.57 ± 4.090 and 13.77 ± 4.888) and *E. coli* group (mean = 29.87 ± 8.334, 25.30 ± 7.550 and 13.70 ± 2.900). Consistent result was obtained by flow cytometry (Figure 2(b)). In practical terms, the proportion of tumor-infiltrating $CD3^+$, $CD4^+$, and $CD8^+$ T cells (mean = 2.088 ± 1.041%, 0.8550 ± 0.3905% and 0.3867 ± 0.2730%) in *B. breve* group were obviously more than that in control group (mean = 0.6550 ± 0.3021%, 0.2200 ± 0.09423% and 0.1050 ± 0.05857%), *L. rhamnosus* group (mean = 1.278 ± 0.4176%, 0.5167 ± 0.1631% and 0.2200 ± 0.1137%) and *E. coli* group (mean = 1.128 ± 0.7325%, 0.4867 ± 0.3334% and 0.2117 ± 0.1485%). Interestingly, the ratio of $CD4^+/CD3^+$ cells and $CD8^+/CD3^+$ cells showed no difference between the four independent groups (Figure 2(c)), indicating that *B. breve*'s influence to TILs was an increase of quantity. These results suggested *B. breve* promoted local immune in tumor microenvironment.

## *B. breve* primed recruitment of intestinal DCs

To investigate how the oral administration of *B. breve* exerts antitumor effect, we assess its effect on intestinal immune system, where was its resident site. An *in situ* ligated intestine loop model was established. Immunofluorescence test showed *B. breve* induced more $CD11c^+$ DCs (6.778 ± 2.476% compared to 4.196 ± 2.185%, 4.956 ± 2.087%, 4.013 ± 2.270% in the other groups) migrating into ileum villi (Figure 3(a)). Flow cytometric analysis further confirmed this result, and there were more total DCs (defined as $CD11c^+MHC\text{-}II^{hi}$) in ileal lamina propria from *B. breve* group (mean = 1.168 ± 0.5222%) than

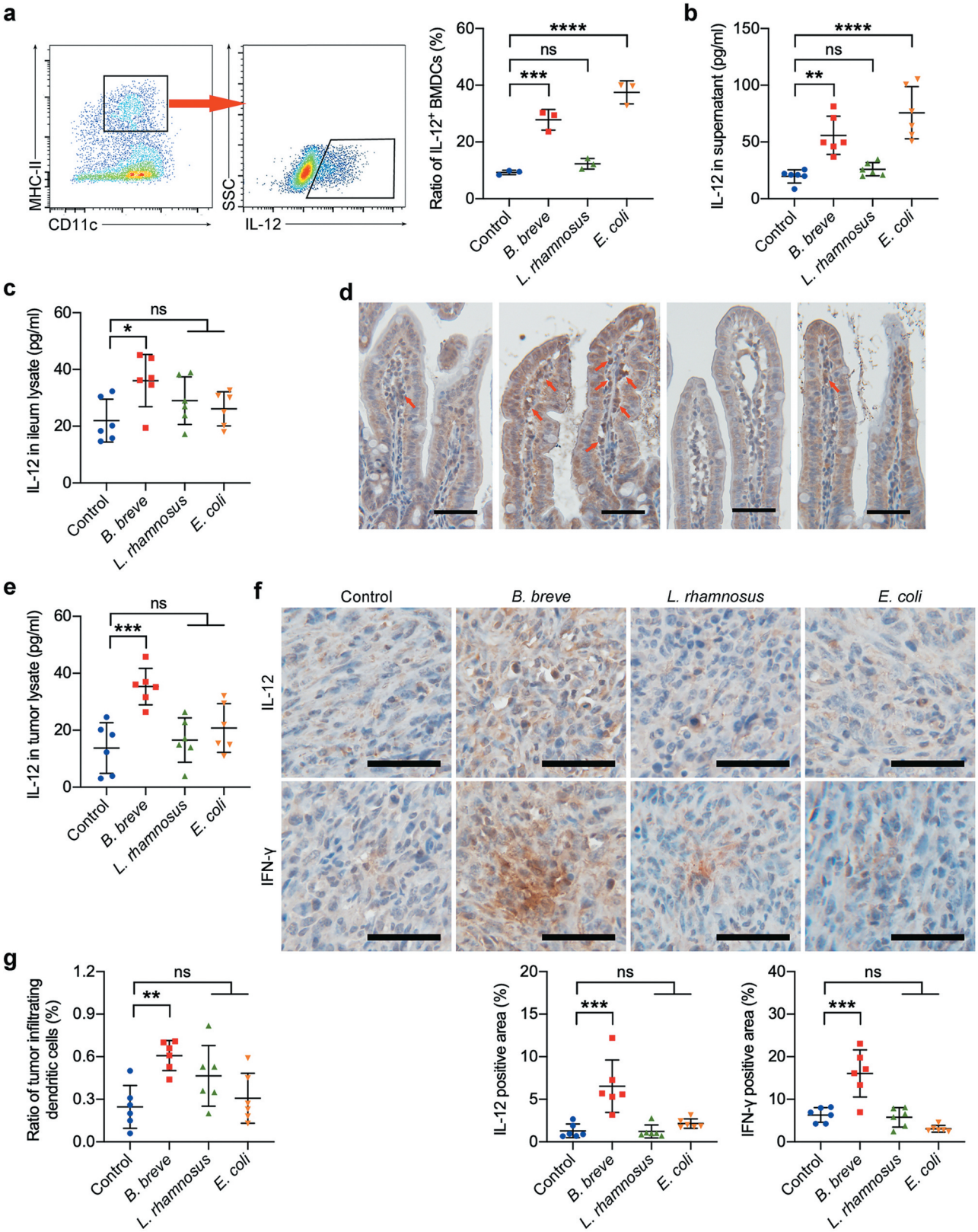


**Figure 5.** ***B. breve*** **derived antitumor effect involved IL-12. a** and **b**. BMDCs were stimulated with medium alone or with *B. breve, L. rhamnosus* or *E. coli* containing medium at a ratio of 1:100 BMDCs to bacterial cells. Representative plots showing gating strategy of $CD11c^{+}MHC\text{-}II^{hi}IL\text{-}12^{+}$ cells within the BMDCs after 8 hours stimulation, as assessed by flow cytometry (**a**, left). The statistical analysis was shown in scatter plots. Each dot represents one sample in two independent experiments (**a**, right; n = 3/group). IL-12 level in the culture supernatant from BMDCs after 24 hours stimulation, as detected by ELISA. Each dot represents one sample in two independent experiments (**b**; n = 3/group). **c** and **d**. Ligated loops of C3H/HeN mice were injected with PBS, *B. breve, L. rhamnosus* or *E. coli* for 45 min. IL-12 level in the ileum lysate was detected by ELISA (c). The expression of IL-12 in ileum tissues was detected by immunohistochemical staining assay and IL-12 positive cells were pointed by red arrows (**d**; scale bar: 50 μm). **e**. IL-12 level in the tumor lysate from C3H/HeN mice, as detected by ELISA. **f**. The expressions of IL-12 and IFN-γ in tumor tissues were detected by immunohistochemical staining assay (upper; scale bar: 50 μm). The quantitative analysis was performed by ImageJ software (lower). **g**. The ratio of tumor infiltrating $CD45^{+}CD11c^{+}MHC\text{-}II^{hi}$ DCs of C3H/HeN mice. Each dot represents one mouse in two to three independent experiments of six mice per group (**c, e-g**). All these data were analyzed with one-way ANOVA and presented as mean ± SD (*$P < .05$; **$P < .01$; ***$P < .001$; ****$P < .0001$; ns, not significant).

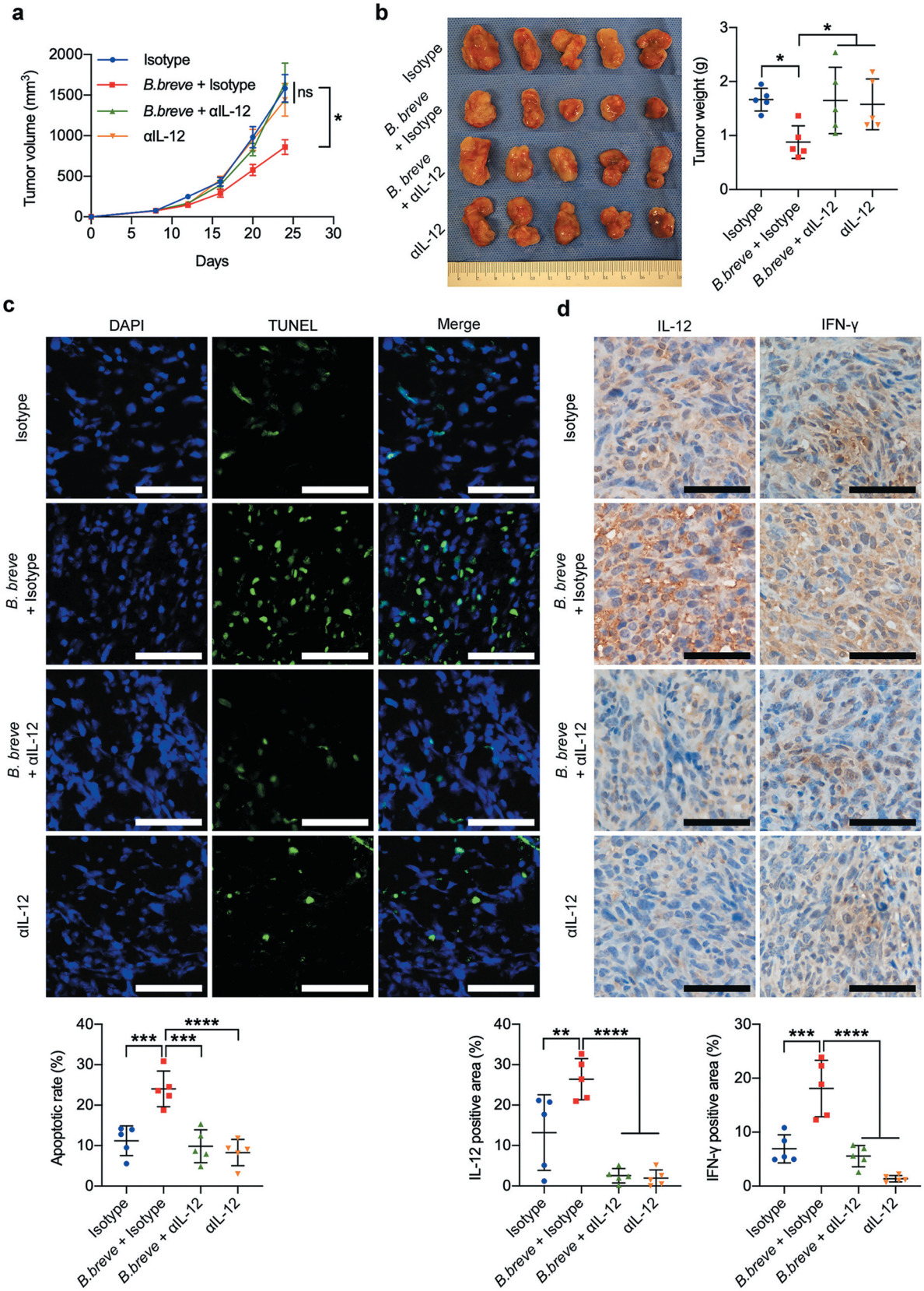


**Figure 6. Antitumor effect of *B. breve* depended on IL-12**. C3H/HeN mice were subcutaneously injected with $3 \times 10^6$ of SCC VII cells. **a**. Tumor growth in C3H/HeN mice treated with PBS and isotype antibody (Isotype, 1 mg/mouse), orally taken *B. breve* ($1 \times 10^9$/mouse) and isotype antibody (*B. breve* + Isotype), neutralizing antibody for IL-12 (αIL-12, 1 mg/mouse) or both of *B. breve* and αIL-12 (*B. breve* + αIL-12). The data was presented as mean ± SEM. **b**. After administration, the tumors were excised (left), and the tumor weight was shown in (right); **c**. Apoptosis of tumor tissues from C3H/HeN mice was assayed with TUNEL staining and observed under fluorescence microscope (upper; scale bar: 50 μm). The quantitative analysis of apoptotic tumor cells was performed by ImageJ software and presented in bar charts (lower). **d**. The expressions of IL-12 and IFN-γ in tumor tissues were detected by immunohistochemical staining assay (upper; scale bar: 50 μm). The quantitative analysis was performed by ImageJ software (lower). Each dot represents one mouse (n = 5/group). Data in **b-d** were presented as mean ± SD. Statistics were two-way ANOVA for tumor-growth curve (a) and one-way ANOVA to compare four independent groups (**b-d**; *$P$ < .05; **$P$ < .01; ***$P$ < .001; ****$P$ < .0001; ns, not significant).

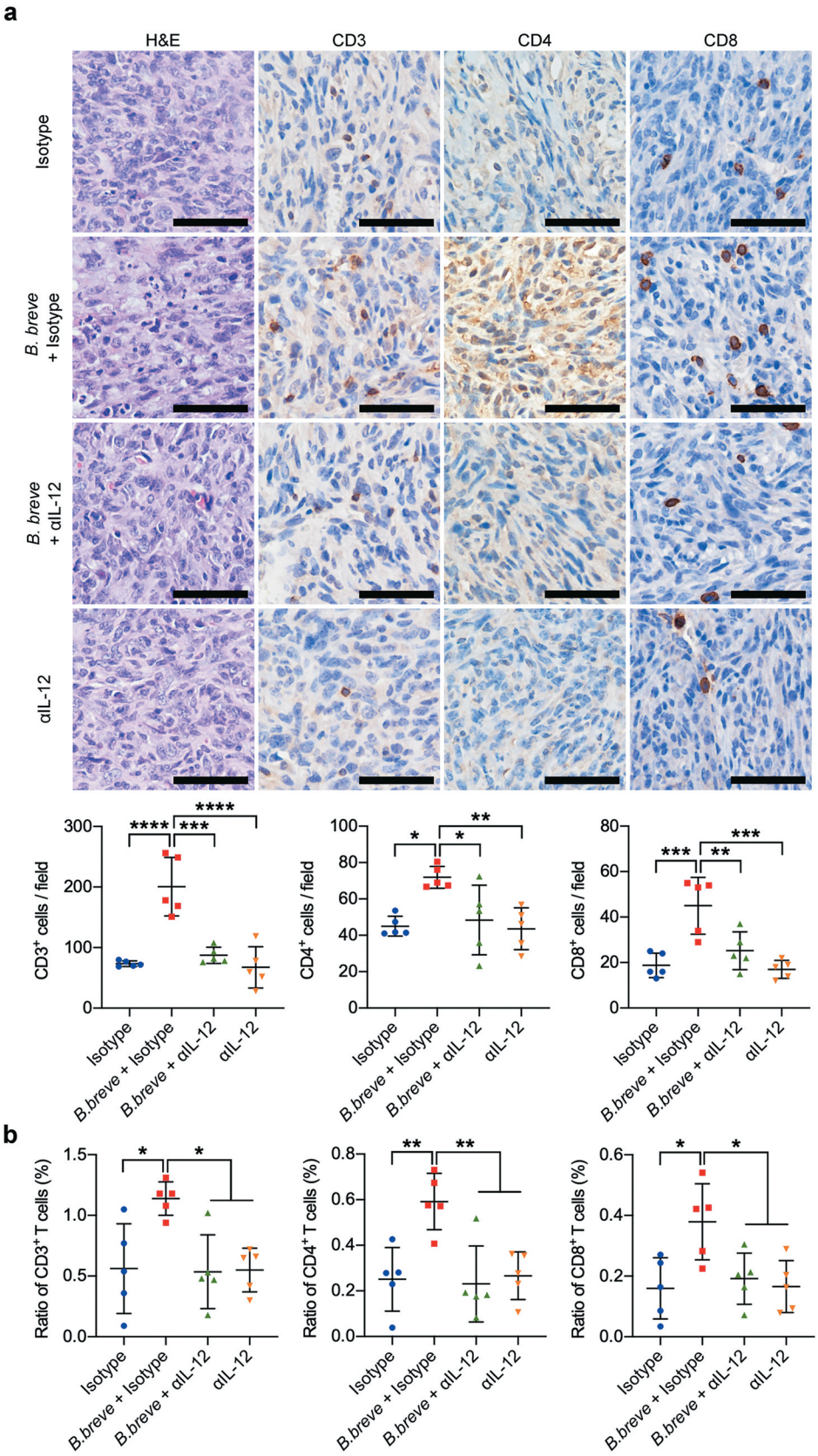


**Figure 7. IL-12 blocking counteracted the increase of TILs derived from *B. breve* treatment. a**. Representative H&E staining images of tumor tissues were shown in the left panel, and the expressions of CD3, CD4, and CD8 in tumor tissues were detected by immunohistochemical staining assay (upper; scale bar: 50 μm). The quantitative analysis was performed by ImageJ software and the number of positive cells were presented in scatter plots (lower). **b**. Percentage of $CD3^+$, $CD4^+$, and $CD8^+$ T cells within the tumor of C3H/HeN mice from each group were assessed by flow cytometry and the statistical analysis was shown in scatter plots. Each dot represents one mouse (n = 5/group). All these data were analyzed with one-way ANOVA and presented as mean ± SD (*$P < .05$; **$P < .01$; ***$P < .001$; ****$P < .0001$).

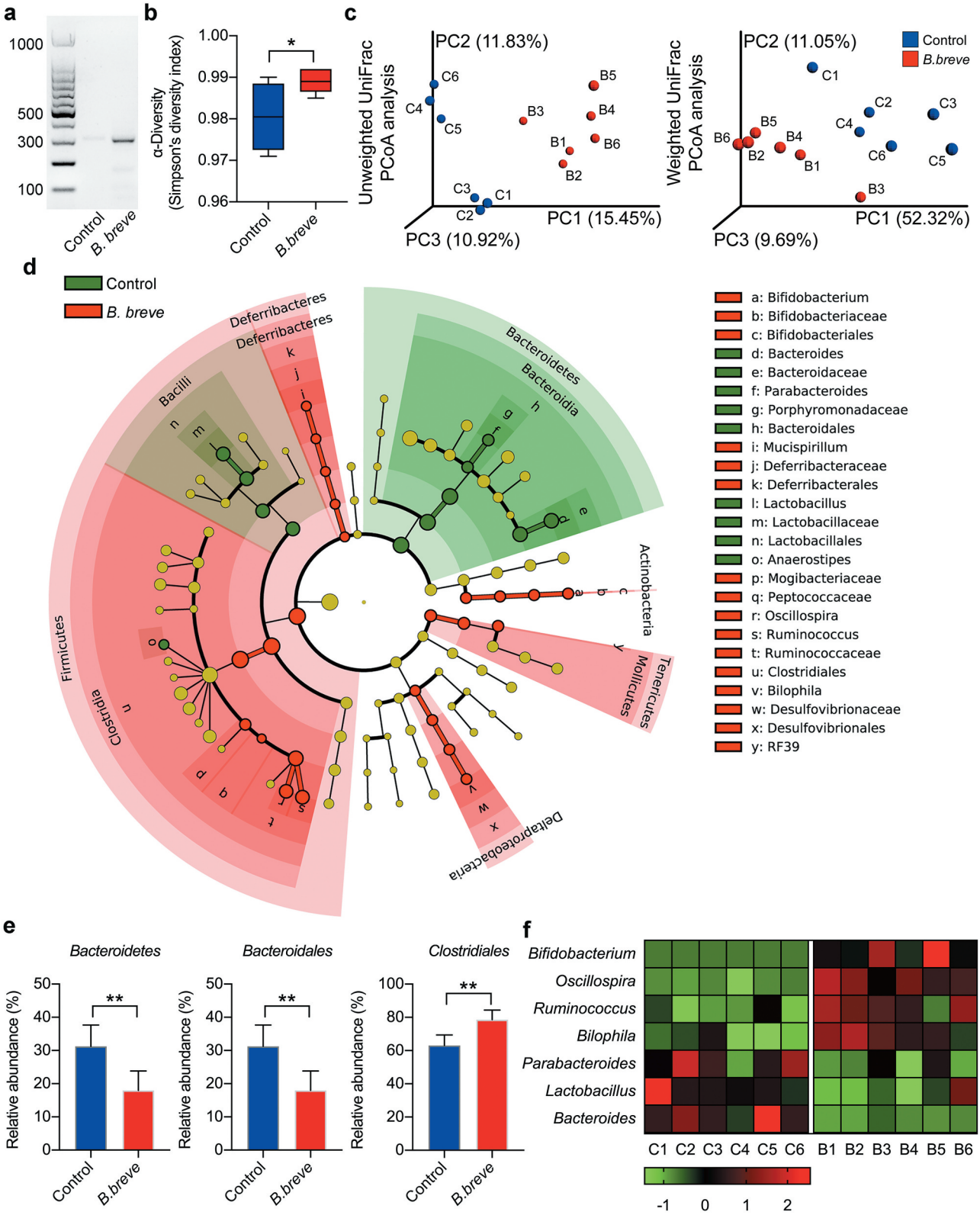


**Figure 8. Oral administration of *B. breve* modulated intestinal microbiota in C3H/HeN mice**. The C3H/HeN mice were administrated by gavage with PBS (control) or *B. breve* every other day and the intestinal contents were collected after 2–3 weeks to detect the intestinal microbiota. C1, C2, C3, C4, C5, and C6 belonged to the control group, B1, B2, B3, B4, B5, and B6 belonged to the experimental group. **a**. The relative abundance of *B. breve* was detected by PCR. **b**. Alpha diversity (Simpson's diversity index) of the two group. **c**. Three-dimension ordination group of unweighted and weighted UniFrac PCoA analysis, in which distances between the samples represented the differences of them. **d**. The classification tree of different species between the two groups based on LEfSe. **e**. At the phylum level, the abundance of *Bacteroidetes* was analyzed. At the order level, the abundances of *Bacteroidales* and *Clostridiales* were analyzed. **f**. The heatmap with normalization of relative abundance at the genus level was indicated from green (less) to red (more). All these data were analyzed with two tailed Student's *t* test and presented as mean ± SD (*$P < .05$; **$P < .01$).

the other groups (mean = 0.4200 ± 0.2667%, 0.6000 ± 0.3678% and 0.4560 ± 0.4084%). Subpopulation analysis indicated that intestinal DCs composed mostly of $CD103^{-}CD11b^{+}$ DCs, which was the only subset (distinguished by CD103 and CD11b) changed between *B. breve* group and the other groups (Figure 3(b)). Correspondingly, CCL20 as the chemokine attracting immature DCs, was upregulated in the intestinal epithelium of *B. breve*-treated mice (9.263 ± 6.275% compared to 1.501 ± 1.879%, 2.700 ± 5.056%, 3.237 ± 3.880% in the other groups, Figure 3(c)). The same result was examined by qRT-PCR as well (Figure 3(d)). Moreover, qRT-PCR results demonstrated mRNA expression level of TLR2 in *B. breve* group was obviously higher than the other groups (Figure 3(e). Furthermore, the mRNA expression level of TLR2's adaptor TIRAP and TRAF6, an essential downstream molecular, were also upregulated after *B. breve* treatment (Figure 3(f)). These indicated that TLR signaling might be activated by *B. breve*. Collectively, *B. breve* stimulated intestinal epithelium to express CCL20 and recruit DCs.

### *B. breve promoted BMDC maturation in vitro*

As the most powerful and professional antigen-presenting cells (APC), DCs' main function is to process and present antigen to T cells. To better understand DCs' changes derived from *B. breve*'s stimulation, the expression level of APC response-related genes was evaluated by qRT-PCR. The expression of Relb, which was one of the most primary transcription factors associated with DC development and maturation was upregulated (Figure 4(a)). Il-12a and Il-12b genes encoded the subunits of IL-12, a bridge cytokine that connected DCs and T cells, were significantly upregulated (approximately 10 times) after *B. breve*'s treatment (Figure 4(b)). Antigen processing related genes, Rab27a, Slc11a1 and Tapbp, were also upregulated in *B. breve* group (Figure 4(c)). It was remarkable that vital co-stimulatory molecules, especially CD40 and CD70, were upregulated due to *B. breve* intervention (Figure 4(d)). Some crucial genes in type I interferon signaling also exhibited upregulation (Figure 4(e)). Then apart from these, expression of Th1-type chemokines CX3CL1 and CXCL9 also increased in *B. breve* group (Figure 4(f)). Compared with control group, *L. rhamnosus* treatment didn't exhibit significant promotion effect on BMDC maturation. But *E. coli* group showed similar results as *B. breve* group. In summary, direct stimulation of *B. breve* was able to induce BMDC to become mature and prime the antigen processing-related genes and signaling.

### *The antitumor effect was related with IL-12*

Based on the above qRT-PCR results, we investigated the role of IL-12, which might play a key role in *B. breve*'s antitumor effect. After stimulated by *B. breve* for 8 hours, an increasing number of IL-12-positive DCs were detected by flow cytometry (27.83 ± 3.623% compared to 9.270 ± 0.7654% in control group and 12.33 ± 1.872% in *L. rhamnosus* group, Figure 5(a)). The ELISA result also showed that there were much more IL-12 secreted into the supernatant from DCs, which were co-cultured with *B. breve* for 24 hours (55.84 ± 16.84 pg/ml compared to 19.78 ± 5.826 pg/ml in control group and 26.04 ± 5.882 pg/ml in *L. rhamnosus* group, Figure 5(b)). Similarly, *E. coli* treatment caused more expression of IL-12 in BMDCs *in vitro* (Figure 5(a,b)). Furthermore, the *in vivo* expression of IL-12 in ileum and tumor tissues were measured using ELISA and immunohistochemistry. After stimulated by three kinds of bacteria for 45 minutes, the expression level of IL-12 in ligated ileum was only upregulated significantly in the *B. breve* groups (mean = 36.10 ± 9.210 pg/ml, compared to 21.98 ± 7.561 pg/ml in control, Figure 5(c)). Immunohistochemistry staining showed consistent results in Figure 5(d). Tumors from the *B. breve* gavage group expressed more IL-12 (mean = 35.34 ± 6.409 pg/ml) than the other groups (mean = 13.77 ± 8.892 pg/ml, 16.56 ± 7.810 pg/ml and 20.81 ± 8.541 pg/ml, Figure 5(e)). A more direct evidence was obtained via immunohistochemical analysis. As shown in Figure 5(f), the positive area of IL-12 in *B. breve*-treated mice was increased over 5 times (6.543 ± 3.078% in *B. breve* group and 1.298 ± 0.8132% in control group). Meanwhile, the expression of IFN-γ was also increased significantly (mean = 16.07 ± 5.550%) compared to control group (mean = 6.319 ± 1.721%), which indicated the activation of T cell-DC crosstalk. Furthermore, we found that there were more infiltrating DCs in tumors of C3H/HeN mice from *B. breve* group (0.6083 ± 0.1057% compared to 0.2467 ± 0.1515% in control group, Figure 5(g)), which indicated more powerful antitumor immuno-microenvironment. These changes were not detected in either *L. rhamnosus* group or *E. coli* group. From above, the antitumor effect derived from *B. breve* involved cytokine IL-12.

### Antitumor effect of *B. breve* depended on IL-12

To further excavate the vital role of IL-12 in the *B. breve*-derived antitumor efficacy, we used a neutralizing antibody for IL-12 (αIL-12) in tumor-bearing mice that received *B. breve* gavage. As shown in Figure 6(a,b), the tumor inhibition effect was counteracted because of αIL-12 treatment. TUNEL assay displayed more apoptotic cells in tumor tissues treated with *B. breve* (mean = 24.02 ± 4.394%), while αIL-12 counteracted this phenomenon as its in isotype group (9.862 ± 4.086% and 11.21 ± 3.655%, Figure 6(c)). The expression level of IFN-γ was also decreased (Figure 6(d)). Correspondingly, the effect of *B. breve* treatment upon T cell infiltration was also vanished, compared with the mice that didn't receive the neutralizing antibody (Figure 7(a,b)). Above results validated that oral administration of *B. breve* promotes antitumor efficacy via DCs derived IL-12.

### *The modulation of intestinal microbiota was triggered by B. breve*

Considering the administration way of *B. breve*, it was natural to take into account that whether there was increase of *B. breve* colonization in gut and the corresponding change of intestinal microbiota. Universal primers of *B. breve*'s 16S ribosomal RNA was designed to evaluate the relative abundance of *B. breve* in the intestinal contents by PCR. As shown in Figure 8(a), there were obviously more *B. breve* colonizing in gut of mice from experimental group. We assessed the general landscape of the

intestinal microbiota on mice from control and *B. breve*-treated group. According to Simpson's Diversity Index, there was a noticeable increase biodiversity of intestinal flora since the intervention (Figure 8(b)), which always stands for beneficial immune status. Principal Coordinates Analysis (PCoA) is a method to explore and to visualize similarities or dissimilarities of data. Through this method, a clearly distinguishable clustering between control and experimental group was revealed by both unweighted and weighted UniFrac PCoA analysis (Figure 8(c)), suggesting that intestinal microbial community structure notably changed after *B. breve* administration. To further investigate the changes of intestinal microbiota, we used LEfSe (Linear discriminant analysis Effect Size) analysis, which detected marked differences in the predominance of bacteria communities between the two groups. Generally, the classification tree exhibited the hierarchical relationship among all taxonomic units from phylum to genus (Figure 8(d)). In brief, treatment of *B. breve* downregulated *Bacteroidetes* at phylum level and *Bacteroidales* at order level, and upregulated *Clostridiales* at order level (Figure 8(e)). Meanwhile, 7 kinds of bacteria showed visible difference. After *B. breve* administration, the abundances of the *Oscillospira* genus in the Firmicutes phylum was significantly upregulated, whereas the abundance of the *Bacteroides* genus in the Bacteroidetes phylum was downregulated (Figure 8(f)). All of these results suggested that *B. breve* could modulate intestinal microbiota.

## Discussion

Altogether, our findings indicated that *B. breve* could significantly inhibit the growth of transplanted tumors in C3H/HeN mice, which relied on the recruitment of intestinal DCs and TILs in tumor microenvironment. IL-12 secreted by DCs played a crucial role in this process. To clear the distinct antitumor effect of *B. breve*, we chose *L. rhamnosus* and *E. coli* as control bacteria. Compared with *B. breve, L. rhamnosus* administration caused completely different results. Whether *in vivo* or *in vitro, L. rhamnosus* couldn't prime antitumor immunity. Interestingly, *E. coli* could promote BMDC maturation as *B. breve in vitro* (Figures 4, 5 (a,b)), but couldn't exert antitumor effect by oral administration *in vivo* (Figures 1 and 2). We found the main reason for this phenomenon was that *E. coli* couldn't prime recruitment of DCs into intestinal villi (Figure 3). Therefore, the priming process of antitumor immunity from *B. breve* composed of recruitment and maturation of DCs, which couldn't be caused by *L. rhamnosus* or *E. coli*.

Furthermore, we put our efforts on the detailed mechanisms of the antitumor effect derived from orally taken *B. breve* in tumor microenvironment. Previous studies[35,36] have divided solid tumors into two kinds: "hot" tumor and "cold" tumor. The former, with more TILs, usually hold better therapy responses and clinical prognosis, and researchers tried to make "cold" tumor "hot" these days. In our study, oral administration of *B. breve* brought more TILs, which would be one useful way to change "cold" tumor to "hot" one. This result was also consistent with the research that intestinal *Bifidobacterium* promoted the efficacy of PD-L1 antibody against melanoma.[25]

The extraintestinal tumors are, in a sense, a kind of distal organs, and how the bacteria in intestines could exert such distal tumor inhibition effect in other sites beyond the gut? It was reported that, *Clostridium* species recruited hepatic $CXCR6^+$ NKT cells against liver tumors.[37] There were also several studies focusing on the interaction between specific bacteria and T cells.[23–25] In addition, the interaction between *Bifidobacterium* and intestinal DCs was also reported in studies.[25,38,39] In this study, we focused on the response of intestinal DCs after *B. breve* taken orally and explored further mechanism especially, for which were not clearly elucidated till now. Our results showed that there were more DCs migrating into ileum villi through activation of TLR signaling pathway and upregulation of CCL20 in the intestinal epithelium, which made their interaction possible. More detailed analysis indicated that intestinal DCs composed mostly of $CD103^-CD11b^+$ migratory DCs (Figure 3(b)), which was reported to be superior to both $CD103^+$ $CD11b^-$ and $CD103^+$ $CD11b^+$ migratory DCs in inducing IFN-γ production by T cells.[40]

Moreover, BMDCs' functions, including antigen processing, $CD8^+$ T cells activation and co-stimulation, and immune cells recruitment, were activated by *B. breve* stimulation *in vitro*, which evidenced the *in vivo* procession indirectly. However, such as which part of *B. breve* (DNA or exopolysaccharides) mediate the interaction between intestinal DCs and *B. breve* in gut is still unclear, which we are currently investigating.

SCC VII cell line was proofed to be poorly immunogenic and resistant to tumor-specific T-cell therapy both *in vivo* and *in vitro*, which means it lacks of tumor neoantigens,[41] but *B. breve* still triggered significant antitumor effect. In *B. breve* treated BMDC group, some important co-stimulation molecules were up-regulated obviously, such as CD40 and CD70. CD40 could license dendritic cells to promote antitumor T cell activation,[42] and CD70 was an essential signaling molecule on membrane of DCs to maintain proper pro-inflammatory Th1 responses.[43] Meanwhile, we found *B. breve* treatment promoted DCs to produce more IL-12, which would stimulate and strengthen antitumor T cell immunity. And more expression of IL-12 was closely related to the upregulation of CD40 in DCs.[19] More importantly, higher IL-12 level within both of ileum and tumor tissues might suggest that the secretion and circulation of IL-12 connect intestinal immune regulation and distal antitumor responses, though we didn't achieve more direct proof. It was also explained by this deduction why similar tumor inhibition results could be observed in CT26. WT tumors of BALB/c mice (supplementary figure S2). Furthermore, the neutralizing antibody for IL-12 completely counteracted the antitumor efficacy derived from oral *B. breve* in mice and brought a serious of changes, concluding decrease of TILs and downregulation of IFN-γ. All above, an important finding of this study is that the probiotic bacteria *B. breve* could produce an antitumor immune response based on DCs-derived IL-12, which not relied on the presence of neoantigen. Hence, *B. breve* can be more widely used in antitumor immunity or as immune adjuvant.

A recent study[22] declared the close relationship among $CD103^+CD11b^-$Batf3-dependent cDC1, IL-12 and

immunogenic commensals, which was important to the chemotherapy-induced antitumor immune response in colon cancer. Combining our results, migratory DCs and IL-12 played crucial roles in intestinal immunity whether in terminal ileum or colon. An interesting point is the difference of the contributing DC subset between the two studies, which might offer a new sight for the research of DC subsets in intestinal lamina propria.

In consideration of the administration method, we investigated the diversities and the structural features of intestinal microbiota. *Oscillospira* is an enigmatic bacterial genus that has never been cultured, but recent evidence suggested that it was positively associated with host health.[44] It has been reported that *Bacteroides* can induce Treg cells and some species can secret a carcinogenic molecule, zinc-dependent metalloprotease toxin.[45] Its down-regulation might make positive contribution to the antitumor effect. We haven't found relative reports about tumor involved the other five kinds of bacteria.

In conclusion, our study evidenced probiotic *B. breve* can trigger tumor apoptosis and inhibit tumor growth in mice. The mechanism relies on recruitment of intestinal DCs and up-regulation of IL-12, which promotes the recruitment of T cells to tumor microenvironment. Moreover, the modulation of gut microbiota caused by exogenous *B. breve* might enhance its antitumor effect. This study provides a simple and easy way to promote antitumor immunity via *B. breve*.

## Disclosure of Potential Conflicts of Interest

The authors declare no conflict of interest.

## Funding

This research was funded by National Natural Science Foundation of China (81672664, 81802699, 81972540).

## ORCID

Qingxiang Li http://orcid.org/0000-0003-2343-8382
Yuke Li http://orcid.org/0000-0002-6334-3655
Yifei Wang http://orcid.org/0000-0002-6509-7726
Le Xu http://orcid.org/0000-0002-4089-3427
Yuxing Guo http://orcid.org/0000-0003-3564-7173
Yixiang Wang http://orcid.org/0000-0001-5291-9826
Chuanbin Guo http://orcid.org/0000-0001-5810-824X

## References

1. Cramer JD, Burtness B, Le QT, Ferris RL. The changing therapeutic landscape of head and neck cancer. Nat Rev Clin Oncol. 2019;16:669–683. doi:10.1038/s41571-019-0227-z.
2. Oosting SF, Haddad RI. Best practice in systemic therapy for head and neck squamous cell carcinoma. Front Oncol. 2019;9:815. doi:10.3389/fonc.2019.00815.
3. Turksma AW, Braakhuis BJ, Bloemena E, Meijer CJ, Leemans CR, Hooijberg E. Immunotherapy for head and neck cancer patients: shifting the balance. Immunotherapy. 2013;5:49–61. doi:10.2217/imt.12.135.
4. Rowshanravan B, Halliday N, Sansom DM. CTLA-4: a moving target in immunotherapy. Blood. 2018;131:58–67. doi:10.1182/blood-2017-06-741033.
5. Oliva M, Spreafico A, Taberna M, Alemany L, Coburn B, Mesia R, Siu LL. Immune biomarkers of response to immune-checkpoint inhibitors in head and neck squamous cell carcinoma. Ann Oncol. 2019;30:57–67. doi:10.1093/annonc/mdy507.
6. Wei SC, Levine JH, Cogdill AP, Zhao Y, Anang NAS, Andrews MC, Sharma P, Wang J, Wargo JA, Pe'er D, et al. Distinct cellular mechanisms underlie anti-CTLA-4 and anti-PD-1 checkpoint blockade. Cell. 2017;170:1120–33.e17. doi:10.1016/j.cell.2017.07.024.
7. Feldman SA, Assadipour Y, Kriley I, Goff SL, Rosenberg SA. Adoptive cell therapy–tumor-infiltrating lymphocytes, T-cell receptors, and chimeric antigen receptors. Semin Oncol. 2015;42:626–639. doi:10.1053/j.seminoncol.2015.05.005.
8. Palucka K, Banchereau J. Dendritic-cell-based therapeutic cancer vaccines. Immunity. 2013;39:38–48. doi:10.1016/j.immuni.2013.07.004.
9. Huang AC, Postow MA, Orlowski RJ, Mick R, Bengsch B, Manne S, Xu W, Harmon S, Giles JR, Wenz B, et al. T-cell invigoration to tumour burden ratio associated with anti-PD-1 response. Nature. 2017;545:60–65. doi:10.1038/nature22079.
10. Rizvi NA, Hellmann MD, Snyder A, Kvistborg P, Makarov V, Havel JJ, Lee W, Yuan J, Wong P, Ho TS, et al. Cancer immunology. Mutational landscape determines sensitivity to PD-1 blockade in non-small cell lung cancer. Science. 2015;348:124–128. doi:10.1126/science.aaa1348.
11. Vetizou M, Pitt JM, Daillere R, Lepage P, Waldschmitt N, Flament C, Rusakiewicz S, Routy B, Roberti MP, Duong CP, et al. Anticancer immunotherapy by CTLA-4 blockade relies on the gut microbiota. Science. 2015;350:1079–1084. doi:10.1126/science.aad1329.
12. Matson V, Fessler J, Bao R, Chongsuwat T, Zha Y, Alegre ML, Luke JJ, Gajewski TF. The commensal microbiome is associated with anti-PD-1 efficacy in metastatic melanoma patients. Science. 2018;359:104–108. doi:10.1126/science.aao3290.
13. Derosa L, Hellmann MD, Spaziano M, Halpenny D, Fidelle M, Rizvi H, Long N, Plodkowski AJ, Arbour KC, Chaft JE, et al. Negative association of antibiotics on clinical activity of immune checkpoint inhibitors in patients with advanced renal cell and non-small-cell lung cancer. Ann Oncol. 2018;29:1437–1444. doi:10.1093/annonc/mdy103.
14. Sen S, Carmagnani Pestana R, Hess K, Viola GM, Subbiah V. Impact of antibiotic use on survival in patients with advanced cancers treated on immune checkpoint inhibitor phase I clinical trials. Ann Oncol. 2018;29:2396–2398. doi:10.1093/annonc/mdy453.
15. Dong M, Meng Z, Kuerban K, Qi F, Liu J, Wei Y, Wang Q, Jiang S, Feng M, Ye L. Diosgenin promotes antitumor immunity and PD-1 antibody efficacy against melanoma by regulating intestinal microbiota. Cell Death Dis. 2018;9:1039. doi:10.1038/s41419-018-1099-3.
16. Teng MW, Bowman EP, McElwee JJ, Smyth MJ, Casanova JL, Cooper AM, Cua DJ. IL-12 and IL-23 cytokines: from discovery to targeted therapies for immune-mediated inflammatory diseases. Nat Med. 2015;21:719–729. doi:10.1038/nm.3895.
17. Vom Berg J, Vrohlings M, Haller S, Haimovici A, Kulig P, Sledzinska A, Weller M, Becher B. Intratumoral IL-12 combined with CTLA-4 blockade elicits T cell-mediated glioma rejection. J Exp Med. 2013;210:2803–2811. doi:10.1084/jem.20130678.
18. Floros T, Tarhini AA. Anticancer cytokines: biology and clinical effects of interferon-alpha2, interleukin (IL)-2, IL-15, IL-21, and IL-12. Semin Oncol. 2015;42:539–548. doi:10.1053/j.seminoncol.2015.05.015.
19. Garris CS, Arlauckas SP, Kohler RH, Trefny MP, Garren S, Piot C, Engblom C, Pfirschke C, Siwicki M, Gungabeesoon J, et al. Successful anti-PD-1 cancer immunotherapy requires T cell-dendritic cell crosstalk involving the cytokines IFN-gamma and IL-12. Immunity. 2018;49(1148–61.e7):1148–1161.e7. doi:10.1016/j.immuni.2018.09.024.
20. Lin L, Rayman P, Pavicic PG Jr., Tannenbaum C, Hamilton T, Montero A, Ko J, Gastman B, Finke J, Ernstoff M, et al. Ex vivo conditioning with IL-12 protects tumor-infiltrating CD8(+) T cells from negative regulation by local IFN-gamma. Cancer Immunol Immunother. 2019;68:395–405. doi:10.1007/s00262-018-2280-3.
21. Uribe-Herranz M, Bittinger K, Rafail S, Guedan S, Pierini S, Tanes C, Ganetsky A, Morgan MA, Gill S, Tanyi JL, et al. Gut

microbiota modulates adoptive cell therapy via CD8alpha dendritic cells and IL-12. JCI Insight. 2018;3. doi:10.1172/jci.insight.94952.
22. Roberti MP, Yonekura S, Duong CPM, Picard M, Ferrere G, Tidjani Alou M, Rauber C, Iebba V, Lehmann CHK, Amon L, et al. Chemotherapy-induced ileal crypt apoptosis and the ileal microbiome shape immunosurveillance and prognosis of proximal colon cancer. Nat Med. 2020;26:919–931. doi:10.1038/s41591-020-0882-8.
23. Routy B, Le Chatelier E, Derosa L, Duong CPM, Alou MT, Daillere R, Fluckiger A, Messaoudene M, Rauber C, Roberti MP, et al. Gut microbiome influences efficacy of PD-1-based immunotherapy against epithelial tumors. Science. 2018;359:91–97. doi:10.1126/science.aan3706.
24. Li J, Sung CY, Lee N, Ni Y, Pihlajamaki J, Panagiotou G, El-Nezami H. Probiotics modulated gut microbiota suppresses hepatocellular carcinoma growth in mice. Proc Natl Acad Sci USA. 2016;113:E1306–15. doi:10.1073/pnas.1518189113.
25. Sivan A, Corrales L, Hubert N, Williams JB, Aquino-Michaels K, Earley ZM, Benyamin FW, Lei YM, Jabri B, Alegre ML, et al. Commensal Bifidobacterium promotes antitumor immunity and facilitates anti-PD-L1 efficacy. Science. 2015;350:1084–1089. doi:10.1126/science.aac4255.
26. Fernandez L, Langa S, Martin V, Maldonado A, Jimenez E, Martin R, Rodriguez JM. The human milk microbiota: origin and potential roles in health and disease. Pharmacol Res. 2013;69:1–10. doi:10.1016/j.phrs.2012.09.001.
27. Ruiz L, Delgado S, Ruas-Madiedo P, Sanchez B, Margolles A. Bifidobacteria and their molecular communication with the immune system. Front Microbiol. 2017;8:2345. doi:10.3389/fmicb.2017.02345.
28. Grandy G, Medina M, Soria R, Teran CG, Araya M. Probiotics in the treatment of acute rotavirus diarrhoea. A randomized, double-blind, controlled trial using two different probiotic preparations in Bolivian children. BMC Infect Dis. 2010;10:253. doi:10.1186/1471-2334-10-253.
29. Fanning S, Hall LJ, van Sinderen D. Bifidobacterium breve UCC2003 surface exopolysaccharide production is a beneficial trait mediating commensal-host interaction through immune modulation and pathogen protection. Gut Microbes. 2012;3:420–425. doi:10.4161/gmic.20630.
30. Enomoto T, Sowa M, Nishimori K, Shimazu S, Yoshida A, Yamada K, Furukawa F, Nakagawa T, Yanagisawa N, Iwabuchi N, et al. Effects of bifidobacterial supplementation to pregnant women and infants in the prevention of allergy development in infants and on fecal microbiota. Allergol Int. 2014;63:575–585. doi:10.2332/allergolint.13-OA-0683.
31. Saez-Lara MJ, Gomez-Llorente C, Plaza-Diaz J, Gil A. The role of probiotic lactic acid bacteria and bifidobacteria in the prevention and treatment of inflammatory bowel disease and other related diseases: a systematic review of randomized human clinical trials. Biomed Res Int. 2015;2015:505878. doi:10.1155/2015/505878.
32. Wang L, Vuletic I, Deng D, Crielaard W, Xie Z, Zhou K, Zhang J, Sun H, Ren Q, Guo C. Bifidobacterium breve as a delivery vector of IL-24 gene therapy for head and neck squamous cell carcinoma in vivo. Gene Ther. 2017;24:699–705. doi:10.1038/gt.2017.74.
33. Wang L, Wang Y, Li Q, Tian K, Xu L, Liu G, Guo C. Exopolysaccharide, isolated from a novel strain bifidobacterium breve lw01 possess an anticancer effect on head and neck cancer - genetic and biochemical evidences. Front Microbiol. 2019;10:1044. doi:10.3389/fmicb.2019.01044.
34. Yin Y, Qin T, Wang X, Lin J, Yu Q, Yang Q. CpG DNA assists the whole inactivated H9N2 influenza virus in crossing the intestinal epithelial barriers via transepithelial uptake of dendritic cell dendrites. Mucosal Immunol. 2015;8:799–814. doi:10.1038/mi.2014.110.
35. Sharma P, Allison JP. The future of immune checkpoint therapy. Science. 2015;348:56–61. doi:10.1126/science.aaa8172.
36. Li J, Byrne KT, Yan F, Yamazoe T, Chen Z, Baslan T, Richman LP, Lin JH, Sun YH, Rech AJ, et al. Tumor cell-intrinsic factors underlie heterogeneity of immune cell infiltration and response to immunotherapy. Immunity. 2018;49(178–93.e7):178–193.e7. doi:10.1016/j.immuni.2018.06.006.
37. Ma C, Han M, Heinrich B, Fu Q, Zhang Q, Sandhu M, Agdashian D, Terabe M, Berzofsky JA, Fako V, et al. Gut microbiome-mediated bile acid metabolism regulates liver cancer via NKT cells. Science. 2018;360:eaan5931. doi:10.1126/science.aan5931.
38. Fu L, Song J, Wang C, Fu S, Wang Y. Bifidobacterium infantis potentially alleviates shrimp tropomyosin-induced allergy by tolerogenic dendritic cell-dependent induction of regulatory T cells and alterations in gut microbiota. Front Immunol. 2017;8:1536. doi:10.3389/fimmu.2017.01536.
39. de Kivit S, Kostadinova AI, Kerperien J, Morgan ME, Muruzabal VA, Hofman GA, Knippels LMJ, Kraneveld AD, Garssen J, Willemsen LEM. Dietary, nondigestible oligosaccharides and Bifidobacterium breve M-16V suppress allergic inflammation in intestine via targeting dendritic cell maturation. J Leukoc Biol. 2017;102:105–115. doi:10.1189/jlb.3A0516-236R.
40. Cerovic V, Houston SA, Scott CL, Aumeunier A, Yrlid U, Mowat AM, Milling SW. Intestinal CD103(-) dendritic cells migrate in lymph and prime effector T cells. Mucosal Immunol. 2013;6:104–113. doi:10.1038/mi.2012.53.
41. Khurana D, Martin EA, Kasperbauer JL, O'Malley BW Jr., Salomao DR, Chen L, Strome SE. Characterization of a spontaneously arising murine squamous cell carcinoma (SCC VII) as a prerequisite for head and neck cancer immunotherapy. Head Neck. 2001;23:899–906. doi:10.1002/hed.1130.
42. Tay NQ, Lee DCP, Chua YL, Prabhu N, Gascoigne NRJ, Kemeny DM. CD40L expression allows CD8(+) T cells to promote their own expansion and differentiation through dendritic cells. Front Immunol. 2017;8:1484. doi:10.3389/fimmu.2017.01484.
43. Dhainaut M, Coquerelle C, Uzureau S, Denoeud J, Acolty V, Oldenhove G, Galuppo A, Sparwasser T, Thielemans K, Pays E, et al. Thymus-derived regulatory T cells restrain pro-inflammatory Th1 responses by downregulating CD70 on dendritic cells. Embo J. 2015;34:1336–1348. doi:10.15252/embj.201490312.
44. Konikoff T, Gophna U. Oscillospira: a central, enigmatic component of the human gut microbiota. Trends Microbiol. 2016;24:523–524. doi:10.1016/j.tim.2016.02.015.
45. Sears CL, Geis AL, Housseau F. Bacteroides fragilis subverts mucosal biology: from symbiont to colon carcinogenesis. J Clin Invest. 2014;124:4166–4172. doi:10.1172/JCI72334.